

# Polycube Layouts via Iterative Dual Loops

MAXIM SNOEP, TU Eindhoven, The Netherlands  
 BETTINA SPECKMANN, TU Eindhoven, The Netherlands  
 KEVIN VERBEEK, TU Eindhoven, The Netherlands

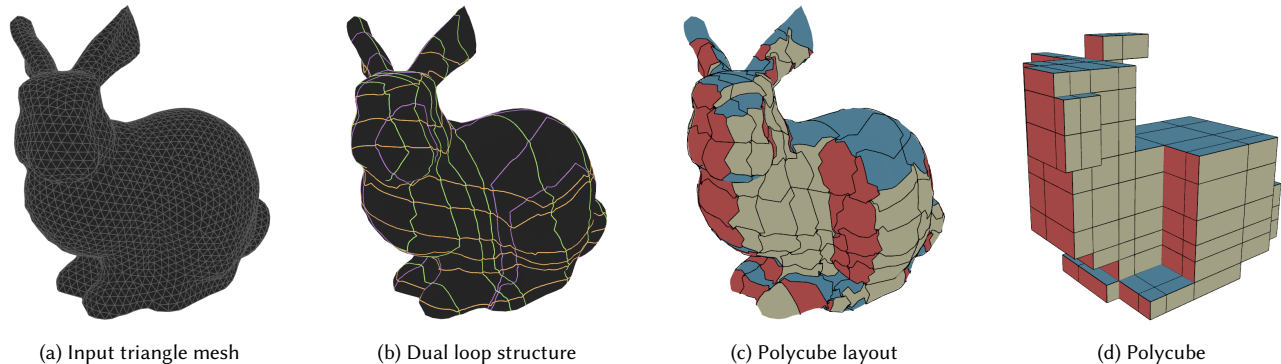


Fig. 1. An iterative approach for the computation of polycube layouts using the dual structure of polycubes.

## ABSTRACT

Polycube layouts for 3D models effectively support a wide variety of methods such as hex-mesh construction, seamless texture mapping, spline fitting, and multi-block grid generation. Our study of polycube layouts is motivated by conformal mesh generation for aerospace modelling. In this setting, quality and correctness guarantees are of the utmost importance. However, currently the fully automatic construction of valid polycube layouts still poses significant challenges: state-of-the-art methods are generally not guaranteed to return a proper solution, even after post-processing, or they use a prohibitively large number of voxels that add detail indiscriminately.

In this paper we present a robust, flexible, and efficient method to generate polycube layouts. Our approach is based on a dual representation for polycube layouts and builds a layout by iteratively adding dual loops. Our construction is robust by design: at any iterative step we maintain a valid polycube layout. We offer the flexibility of manual intervention if the user so desires: while our method is able to compute a complete polycube layout without user intervention, the user can interrupt after each iteration and target further refinement on both the local and the global level. Last but not least, our method is efficient and can be implemented using comparatively simple algorithmic building blocks. Our implementation is publicly available and we present its output for numerous benchmark models.

## 1 INTRODUCTION

Polycubes, or orthogonal polyhedra, are polyhedra with axis-aligned quadrilateral faces. Their simple structure enables efficient methods which are elusive for more general 3D shapes. Hence, so-called polycube maps, which are bijective mappings between general 3D models and polycubes, have been utilized to transfer solutions computed on polycubes into more general settings. Polycube maps have

been used to solve various problems including, but not limited to, texture mapping [Tarini et al. 2004], hexahedral meshing [Pietroni et al. 2022], and structured CFD gridding [Malcevic 2011].

Since polycube maps were introduced in 2004, a variety of methods have been proposed to construct them. Most methods aim to strike a balance between the distortion of the mapping and the complexity of the polycube. The current state-of-the-art achieves a good trade-off between low distortion and low complexity by employing deformation-based approaches [Dumery et al. 2022; Gregson et al. 2011; Livesu et al. 2013]. However, such deformations tend to not be robust: at the end of the deformation there might not be a valid polycube and post-processing might not converge to a valid solution either [Mestrallet et al. 2023; Protais et al. 2022; Sokolov and Ray 2015; Zhao et al. 2019]. Furthermore such methods can generally not be controlled or steered by the user and do not enable flexible refinement or coarsening of the polycube based on user input.

A polycube map between a polycube  $Q$  and a 3D model  $M$  induces a segmentation of  $M$  via the edges of  $Q$ . This segmentation of  $M$  into surface patches is called a polycube layout; it is also referred to as a polycube segmentation, a polycube labeling, or a Cartesian face decomposition. Our motivation to study polycubes and their corresponding polycube layouts stems from conformal mesh generation for aerospace modelling. In this setting the actual polycube is not needed; all that is required is the polycube layout on the input model, which in turn informs the mesh generation around the model. Furthermore, robustness and flexibility are of utmost importance: we always need to create a valid polycube layout and

the users (aerospace engineers) need to be able to interactively add additional detail to the layout as needed for the external mesh.

There are several methods which attempt to directly compute the patches of a polycube layout, and then try to validate this layout by attempting to construct the corresponding polycube. However, when it appears that there is no polycube, then there are few effective remedies. Sometimes local changes can address the issues [Gregson et al. 2011; Livesu et al. 2013], but they are not always effective [Mandad et al. 2022]. Some approaches use the characterization by [Eppstein and Mumford 2010] of certain orthogonal polyhedra to inform their layouts. However, this characterization is rather limited; it includes invalid polycubes and also severely restricts the solution space of possible polycubes [Mandad et al. 2022; Mestrallet et al. 2023; Pietroni et al. 2022].

*Contribution and organization.* We present a robust, flexible, and efficient method to generate polycube layouts for 3D models of genus 0. Our method builds upon the fact that such polycube layouts can be effectively characterized in a dual representation [Baumeister and Kobbelt 2023]. We iteratively build the corresponding dual structure by adding dual loops where needed, all the while maintaining the invariant that the dual structure corresponds to a valid polycube. Our method is robust by design and seamlessly supports user interaction: after each iterative step, the user can choose the next area for iterative refinement. Alternatively, our method is able to compute high quality polycube layouts fully automatically.

After a review of related work in Section 2, we formulate the exact problem statement and our objectives in Section 3. In Section 4 we describe the dual structure and then present the details of our iterative approach in Section 5. We implemented our method and showcase results for numerous benchmark models in Section 6; we believe that the results compare favourably to the state-of-the-art. Finally, in Section 7 we discuss avenues for future work.

## 2 RELATED WORK

In 2004 [Tarini et al. 2004] introduced polycube maps as an extension of cube maps. Polycubes have a simple structure and can easily be parameterized, but still are flexible enough to capture any shape. Due to the versatility of polycube maps, many approaches have been proposed to automate the process of constructing polycubes and the corresponding polycube maps. Early polycube construction methods had significant drawbacks, as they produced polycubes that were either very coarse [Lin et al. 2008] or very detailed [He et al. 2009]. Other methods are only semi-automated and still required a significant amount of user interaction.

The most prominent set of methods for polycube construction is based on a deformation approach which was introduced by [Gregson et al. 2011] and has since been improved or extended by many [Cherchi et al. 2016; Dumery et al. 2022; Fang et al. 2016; Fu et al. 2016; Guo et al. 2020; Huang et al. 2014; Livesu et al. 2013; Mandad et al. 2022; Yang et al. 2019; Yu et al. 2014; Zhao et al. 2019]. The deformation approaches assign a target label to each face on the surface of the input shape, corresponding to the X, Y, and Z axes. Then, the input shape is gradually deformed until the surface faces are oriented toward their assigned target label. This deformation yields a near-polycube: a shape that approximates the axis-aligned

properties of a polycube. However, this near-polycube might have topological inconsistencies that need to be resolved before a valid polycube can be returned. As such, the main drawback of the family of deformation approaches is their robustness: it is often unclear if and how the near-polycube can be transformed into a valid polycube. Several papers use the characterization of orthogonal polyhedra by [Eppstein and Mumford 2010] to establish the validity of a near-polycube, however, this characterization is neither sufficient nor necessary [Mandad et al. 2022; Mestrallet et al. 2023; Pietroni et al. 2022; Sokolov and Ray 2015]. If a deformation method returns a valid polycube then it also directly defines the polycube map between the polycube and the input mesh.

An alternative set of methods is based on voxelization [Wan et al. 2011]. Such methods generally have two drawbacks: the resulting polycube tends to be very detailed, even if that is not desired, and the mapping between the input shape and the polycube is not preserved. Voxelization can also be used to repair the near-polycubes that result from a deformation method [Yang et al. 2019; Yu et al. 2014].

There are also polycube construction methods which explicitly support human interaction. For example, [Wang et al. 2008] allow the user to choose the placement of polycube corners on the input mesh and [Garcia et al. 2013; Xia et al. 2011] support the possibility to sketch desirable features on the input mesh. Recently, [Li et al. 2021] combined both the deformation and the voxelization approach with the possibility for users to edit the individual voxels.

[Biedl and Genc 2004] were the first to characterize orthogonal convex polyhedra (a subset of all polycubes) via their dual structure. Nearly 20 years later, [Baumeister and Kobbelt 2023] independently derived a full combinatorial characterization of all polycubes of genus 0 via their dual loop structure. Our method builds upon this characterization. [Baumeister and Kobbelt 2023] did not use the characterization they derived directly. Instead, they use the (combinatorially much simpler) dual loop structure constructed by [Campen et al. 2012] for quad meshes. These dual loops do not correspond to polycubes and hence [Baumeister and Kobbelt 2023] engage in a local search which eventually turns the quad mesh loop structure into the loop structure of a valid polycube. This process does not take the geometry of the input mesh into account, but focuses exclusively on the combinatorial structure. As a result, the geometry of their final polycubes is generally not similar to that of the input mesh and the mapping distortion between the polycube and the mesh is large; furthermore, there is no apparent possibility during this process to add geometric information. In contrast, we use the dual loop structure directly and iteratively build a valid polycube via controlled loop additions. Hence our method maintains a valid polycube at all times and is able to deliberately add dual loops to minimize distortion and capture the geometry of the input mesh.

## 3 PROBLEM STATEMENT

Our input consists of a 3D model represented by a triangulated mesh  $\mathcal{M} = (V, T)$ , where  $V$  is the set of vertices of the mesh and  $T$  is the set of triangular faces, represented by triples  $(v_i, v_j, v_k)$  of vertices. The edges of the mesh are represented implicitly via the triangles. We assume that  $\mathcal{M}$  is a genus 0 manifold triangle surface mesh, that is,  $\mathcal{M}$  is homeomorphic to the sphere. We briefly discuss

meshes of higher genus in Section 7. Furthermore, we assume that  $\mathcal{M}$  is embedded in  $\mathbb{R}^3$  and that every vertex  $v \in V$  has an associated position  $p(v)$ , and each face  $t \in T$  has an associated normal  $n(t)$ .

A *polycube*  $Q$  is a mesh with quadrilateral faces where the edges of each face are aligned with one of the three principal axes. Alternatively, we can see a polycube as a collection of cubes glued together at their sides. As with the meshes we assume that all polycubes have genus 0. A *polycube map*  $f$  is a bijective mapping between a mesh  $\mathcal{M}$  and a polycube  $Q$ . If we map the edges of  $Q$  back onto  $\mathcal{M}$  (using  $f^{-1}$ ), then we obtain a segmentation of  $\mathcal{M}$ , which we refer to as a *polycube layout*. This polycube layout consists of *patches* that correspond to the faces of  $Q$ , and thus, each has exactly four neighboring patches. In general, a segmentation of a mesh  $\mathcal{M}$  into patches is referred to as a *patch layout*, or a *quad layout* if each patch has exactly four neighboring patches. A patch layout of a mesh  $\mathcal{M}$  is a polycube layout if and only if it corresponds to a polycube map from  $\mathcal{M}$  to some polycube  $Q$ . Note that, in a polycube layout, every patch can be labeled as  $(\pm)X$ ,  $(\pm)Y$ , or  $(\pm)Z$  depending on the direction of the normal of the corresponding face in  $Q$ .

In this paper we focus on computing a high-quality polycube layout for a given input mesh  $\mathcal{M}$ . Given a polycube layout, a polycube map can be computed using various methods [Dumery et al. 2022; Hu and Zhang 2016; Yang et al. 2019; Yu et al. 2014]; such computations are outside the scope of this paper. We also do not focus on a specific quality measure for polycube layouts, as this typically depends on the exact application. Nonetheless, we do take the following general objectives for high quality layouts into account:

- Patches map to quadrilateral faces with low parametric distortion.
- Patches map to orthogonal faces with low angular distortion.
- The layout consists of few patches.

The first two objectives aim for geometric precision: right-angle corners, geodesic arcs, minimal normal deviation, and alignment with axis labels. There is a clear tradeoff between these two objectives and the third objective: layout simplicity. Hence, it should be possible for a user to control this trade-off to obtain the desired result. In fact, for our intended application in conformal mesh generation for aerospace modelling it is important that users can add more detail to the polycube layout where needed.

To fulfill these objectives, we propose an iterative approach to construct polycube layouts, allowing users to stop or intervene in the iterative refinement process. However, iteratively refining the polycube layout directly is challenging: multiple patches must be introduced in a single step, and the resulting patch layout must satisfy not only local conditions but also global conditions to be a valid polycube layout. Therefore, we perform the iterative refinement on the dual structure rather than on the polycube layout itself.

## 4 DUAL STRUCTURE

Consider a polycube  $Q$  and interpret it as a collection of cubes glued together at their sides. Next consider a single *layer*  $\mathcal{L}$  of cubes of  $Q$  along the  $x$ -direction, that is, a subset of all cubes of  $Q$  that contain the same  $x$ -coordinate. This layer  $\mathcal{L}$  may consist of several connected components, so consider one of the connected components  $C$ . We can draw a single loop (closed path) around all

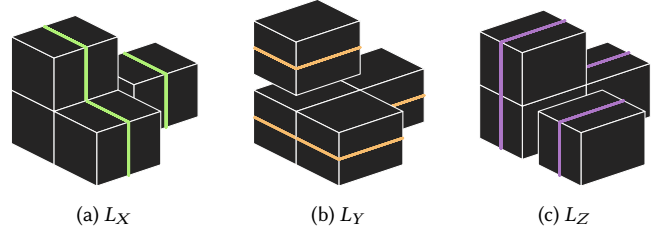


Fig. 2. The three sets of dual loops:  $L_X$  (green),  $L_Y$  (orange), and  $L_Z$  (purple). All sets consist of two loops.

of the cubes in  $C$  that also has the same fixed  $x$ -coordinate as the layer. We refer to such a loop as a *dual loop* of  $Q$ . Let  $L_X$  be the set of dual loops for all layers defined by  $x$ -coordinate, and for all connected components in each layer. Similarly, let  $L_Y$  and  $L_Z$  be the set of dual loops defined by  $y$ -coordinates and  $z$ -coordinates, respectively. We refer to  $(L_X, L_Y, L_Z)$  as the *dual structure* of the polycube  $Q$  (see Fig.2). For any loop  $\ell$  in the dual structure, we say that  $\ell$  has *type*  $X$  if  $\ell \in L_X$  (similarly for  $L_Y$  and  $L_Z$ ).

This dual structure has various nice properties. First of all, an intersection between two dual loops  $\ell_1$  and  $\ell_2$  of different types corresponds to a quadrilateral face of  $Q$ . (Loops of the same type cannot intersect.) Additionally, the types of  $\ell_1$  and  $\ell_2$  determine the orientation of the face. (If  $\ell_1 \in L_X$  and  $\ell_2 \in L_Y$ , then the face is spanned by the  $X$ - and  $Y$ -axis.) Second, every face of the arrangement induced by the loops in the dual structure corresponds to a corner of  $Q$ . We refer to such faces as *dual faces*. The complexity of a dual face corresponds to the number of quadrilateral faces that meet at this corner, and the types of incident loops induce the local structure around the corner.

Now consider a polycube map  $f$  from a mesh  $\mathcal{M}$  to a polycube  $Q$ . By using the inverse map  $f^{-1}$ , we can map the dual structure  $(L_X, L_Y, L_Z)$  of  $Q$  to a (labeled) collection of loops  $(L'_X, L'_Y, L'_Z)$  on  $\mathcal{M}$ . Thus, we also obtain a dual structure on  $\mathcal{M}$ , where the combinatorial structure of the dual loops (intersections and dual faces) is exactly the same as on  $Q$ .

We can try to obtain such a *loop structure* directly starting from the mesh  $\mathcal{M}$  by computing three collections of loops corresponding to the different types. Clearly, not all loop structures correspond to the dual structure of a polycube. [Baumeister and Kobbelt 2023] establish the following necessary and sufficient conditions for a loop structure to correspond to the dual structure of a polycube:

- (1) Two loops of the same type cannot intersect;
- (2) No three loops intersect in the same point;
- (3) The dual faces must be consistent with one of the six possible types of corners, see Fig. 3. Specifically, the complexity of each dual face is between 3 and 6, and at most two loops on the boundary of the face can have the same type;
- (4) Let the *loop complex* of type  $X$  be the graph obtained by having a vertex for each loop  $\ell \in L_X$ , and adding an edge between two vertices if the corresponding loops share a face (if a loop bounds the same face twice, add a self-edge). Similarly, we can construct the loop complexes of types  $Y$  and  $Z$ . The loop complexes of each type must be bipartite.

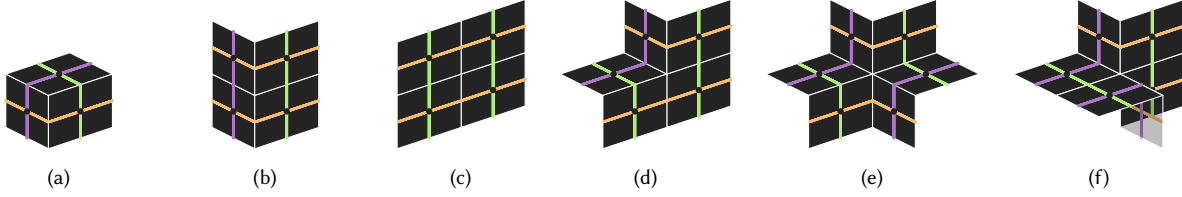


Fig. 3. The six possible corner types of a polycube, characterized by dual loops over the faces of the polycube.

Since our focus lies solely on computing a polycube layout on  $\mathcal{M}$ , we simply refer to a loop structure on  $\mathcal{M}$  with the above properties as a dual structure and denote it as  $(L_X, L_Y, L_Z)$ . As we show in the next section, we can easily compute a valid polycube layout for  $\mathcal{M}$  given a dual structure  $(L_X, L_Y, L_Z)$  on  $\mathcal{M}$ .

## 5 ITERATIVE ALGORITHM

The dual structure enables the following simple iterative algorithm:

- (1) Initialize the dual structure with one loop of each type. Note that each pair of loops must intersect twice. This dual structure corresponds to a polycube consisting of a single cube.
- (2) Repeatedly add a single loop such that the dual structure remains valid.
- (3) *Primalize* the dual structure: construct a polycube layout guided by the dual structure.

Our main contribution in this paper is the generic iterative algorithm described above. However, we still need to make a number of choices to obtain a specific algorithm: How do we compute a new loop to be added to the dual structure? How exactly do we compute the patches of the polycube layout? Also, some variants are possible that still follow the same overall approach. For example, we can add multiple loops instead of a single loop per step, or remove a loop. Also, we may compute the polycube layout in an intermediate step to determine how to compute a new loop to be added to the dual structure. We have implemented our iterative algorithm using a fairly straightforward greedy approach for each of the steps above, which we detail below. We demonstrate in Section 6 that this basic approach already produces good results, showing the versatility of our generic algorithm. However, we will also discuss some possible variants that can be used to further improve the results in Section 7.

### 5.1 Computing loops

We assume that we already have a valid dual structure  $(L_X, L_Y, L_Z)$  on a mesh  $\mathcal{M} = (V, T)$  and that we want to add another loop. Without loss of generality we will simply assume that we want to add a loop  $\ell$  to  $L_X$ , as the other cases are symmetric. In previous work, similar loops have been computed using cross fields [Campen et al. 2012; Livesu et al. 2020; Pietroni et al. 2016], but it is not clear if such loops will often satisfy the requirements of the dual structure. Therefore, we use a more direct approach.

*Loop representation.* We first discuss the representation of a single loop  $\ell$  in the dual structure. Note that, in general,  $\ell$  will not always follow the edges of the mesh, but may pass through the interior of its triangles. Nonetheless, instead of using a geometric (continuous) representation of the loops, we use a combinatorial representation

of the loops. This representation makes it easier to find new loops, easier to interact with, and is also much more efficient. Restricting loops to vertices and edges of the mesh directly is problematic: Condition (1) of a dual structure (Section 4) implies that every vertex and edge can be used by only one loop in  $L_X$ . As we want to ensure that it is always possible to add another loop to the dual structure (to refine the layout further), this representation is not desirable. Instead we construct a type of *edge graph*  $G$ : for every edge  $(u, v)$  in  $\mathcal{M}$  there is a vertex in  $G$ , and two vertices in  $G$  are connected if and only if the two corresponding edges in  $\mathcal{M}$  share a triangle. A loop is then simply represented as a path in  $G$ . In this representation we can allow two loops  $\ell_1$  and  $\ell_2$  of the same type to use the same vertices and edges in  $G$ , as long as they do not properly cross. We can then eliminate the overlap between  $\ell_1$  and  $\ell_2$  in a post-processing step by moving them along the corresponding edges of  $\mathcal{M}$ , which we will describe below. To give the vertices in  $G$  a 3D position (needed for evaluating loops) we simply use the midpoint  $(p(u) + p(v))/2$  of the corresponding edge  $(u, v)$ .

Because we need to know in which order loops of different types cross, we need to store some additional information to represent the entire dual structure. Specifically, we store for every vertex  $u$  in  $G$  (edge in  $\mathcal{M}$ ) the order of the loops passing through  $u$ . If two loops  $\ell_1$  and  $\ell_2$  share the same edge  $(u, v)$  in  $G$  and the order between  $\ell_1$  and  $\ell_2$  is different at  $u$  than at  $v$ , then  $\ell_1$  and  $\ell_2$  must have crossed in the triangle of  $\mathcal{M}$  corresponding to the edge  $(u, v)$  of  $G$ . Using this extra information we can reconstruct the dual structure geometrically when needed (see Fig. 4).

*Loop construction.* To construct a suitable loop  $\ell$  for  $L_X$ , we need to compute a loop on  $\mathcal{M}$  that would be similar to a dual loop of type  $X$  in the resulting polycube. Although  $\ell$  does not strictly need to be constrained to one  $x$ -coordinate (as would be the case in the

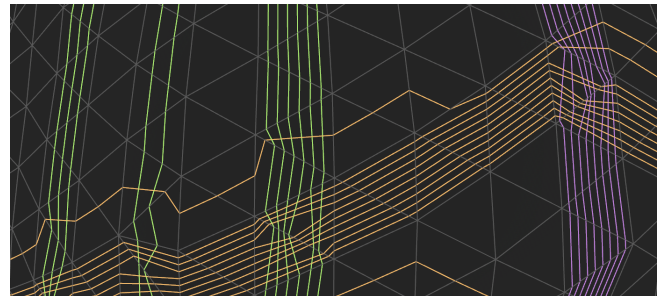


Fig. 4. Using an abstract representation for loops results in the possibility of multiple loops through the same (partial) face sequences.

polycube), it should not vary much in  $x$ -coordinate to ensure low distortion in the corresponding polycube map. We find loops that vary little in  $x$ -coordinate and loop around  $\mathcal{M}$  by formulating the problem as a shortest path problem on a graph  $G_X$ . This graph is obtained by augmenting the graph  $G$  with weights (and making it directed), where the weights are determined by the intended type of the loop ( $X$  in this case). Specifically, consider a directed edge  $e = (u, v)$  in  $G$ , and let  $n(e)$  be the normal vector of the face in  $\mathcal{M}$  that corresponds to  $e$ . Furthermore, let  $a_X(e)$  be the angle between  $(p(v) - p(u)) \times n(e)$  and the unit vector in the positive  $x$ -direction. For some parameter  $\gamma > 0$ , we set the weight of  $e$  to  $w_X(e) = a_X(e)^\gamma$ . Note that this weight can only be zero if  $p(v) - p(u)$  and  $n(e)$  span the  $YZ$ -plane, which encourages shortest paths to follow ridges with a roughly fixed  $x$ -coordinate. Also, if  $w_X(e) = 0$  for some edge  $e = (u, v)$ , then the weight  $w_X(e')$  of the opposite edge  $e' = (v, u)$  is maximal (since  $(p(v) - p(u)) \times n(e)$  will point in the negative  $x$ -direction). This encourages shortest paths to loop around the mesh in a clockwise or counterclockwise direction properly. To compute a potential loop  $\ell$  for  $L_X$ , we can simply pick a vertex  $u$  in  $G_X$  and compute the shortest path from  $u$  to itself in  $G$ . The parameter  $\gamma$  should be set to ensure that the path does not directly turn back to  $u$  without looping around  $\mathcal{M}$ . In our experiments  $\gamma = 1$  is usually sufficient, but  $\gamma$  can be increased if that is not the case.

*Loop selection.* To select the next loop to be added to the dual structure, we simply sample a number of candidate loops as described above (using different starting vertices) for each loop type. We filter out duplicates as well as candidate loops that do not result in a valid dual structure using the conditions described in Section 4. Note that we can easily satisfy some of these conditions already when computing the candidate loops. Specifically, for a particular starting vertex  $u$  in  $G_X$  (for a loop of type  $X$ ), we can use the neighboring loops in  $L_X$  to constrain the shortest path computation from  $u$  to itself in  $G_X$ . As a result, we will typically have enough candidate loops to pick from.

Finally, we select the next loop to be added to the dual structure based on a number of quality measures. For a vertex  $v$  in the mesh  $\mathcal{M}$ , let the *angular defect* be  $\delta(v) = 2\pi - C$ , where  $C$  is the sum of angles (in radians) at  $v$  in incident triangles on  $\mathcal{M}$ . Note that, in a polycube  $Q$ , the number of quadrilaterals meeting in a proper corner of  $Q$  (Fig. 3a/d/e/f) is either 3 or larger than 4, which corresponds to a non-zero angular defect. Thus, we think that vertices of  $\mathcal{M}$  with a large absolute angular defect are good candidates for corners in the polycube layout. For a parameter  $\rho$  ( $0 < \rho < 1$ ), we say that all vertices within the top  $\rho$  fraction of all vertices based on absolute angular defect are *critical* (see Fig. 5). Finally, if we cut the mesh  $\mathcal{M}$  along all loops in  $L_X$ , we refer to the resulting connected components of  $\mathcal{M}$  as *zones* of type  $X$  (similar for  $Y$  and  $Z$ ). We can now define our quality measures for candidate loops:

**Loop length** (maximize) The total (geometric) length of the loop. Longer loops tend to capture more relevant features of the mesh and also impose fewer limitations on future potential loops. This measure is especially relevant for the initial loops.

**Loop distribution** (maximize) The distance to neighboring loops. For loops of type  $X/Y/Z$ , we define this distance as the

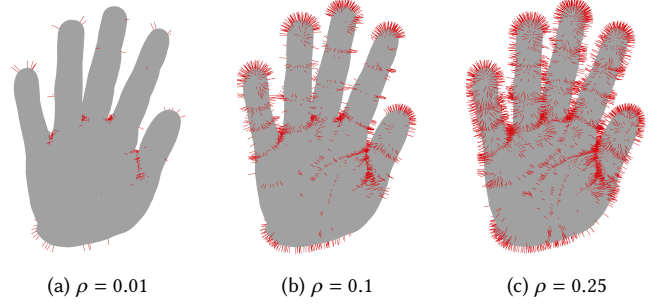


Fig. 5. Critical points on ‘hand040k’ input model.

absolute difference of the average  $x/y/z$ -coordinate between two loops. Loops that are close together often capture the same features and may hence be redundant. By maximizing the distance to neighboring loops we aim to represent as many features as possible with as few loops as possible.

**Critical spread** (minimize) The maximum distance between two critical vertices within a single zone. For zones of type  $X/Y/Z$ , the distance is measured as the absolute difference between  $x/y/z$ -coordinates. Preference is given to loops that separate distant critical vertices from the same zone, as these vertices should not map to the same  $x$ -coordinate in the resulting polycube.

**Critical count** (minimize) The maximum number of critical vertices in a single zone. This measure aims to distribute the critical vertices over different zones, resulting in a balanced and more symmetric distribution.

Each of these quality measures has advantages and can be combined or used independently based on the specific requirements of the mesh and the stage of the iterative process. The effectiveness and comparison of these methods are further elaborated in Section 6.

## 5.2 Primalization

Our final step of the algorithm is to transform the dual structure of  $\mathcal{M}$  into a polycube layout. This step consists of two parts: (1) we select corner vertices for each dual face, and (2) we compute paths on  $\mathcal{M}$  between all adjacent corners that are separated by a single loop. Note that this path must only visit the two dual faces corresponding to the two adjacent corners and cannot intersect with other paths.

To ensure that every dual face contains a potential corner vertex, we first compute a refined mesh  $\mathcal{M}'$  as follows. We first add the loops of the dual structure to  $\mathcal{M}$ , where we use the order of the loops stored in vertices of  $G$  to equally space the loops along the corresponding edge of  $\mathcal{M}$  (see Fig. 4). Next, we further refine some dual faces to ensure that every dual face contains at least one vertex.

*Corner placement.* To construct a polycube layout that is consistent with the computed dual structure of  $\mathcal{M}$ , we need to place exactly one corner per dual face of the dual structure, and we will place this corner on a vertex of  $\mathcal{M}'$ .

Now consider a single zone of type  $X$ . This zone corresponds to a subset of corners in the corresponding polycube that all have

the same  $x$ -coordinate. This leads us to the following desirable properties for corner placements:

**Alignment** Corners that are part of the same zone of type  $X/Y/Z$  should have similar  $x/y/z$ -coordinates.

**Resemblance** Corners with a particular angular defect should be placed on vertices with a similar angular defect.

In our implementation we focus mostly on the alignment aspect, but we reserve a special role for the critical vertices introduced in Section 5.1 to also partially address the resemblance aspect. For each zone of type  $X$ , we determine a target  $x$ -coordinate  $t_x$  for the entire zone by taking a weighted average over all vertices in the zone, where critical vertices have a weight  $W > 1$ , and non-critical vertices have weight 1.  $W$  is a parameter that controls how important the critical vertices are in determining the target coordinate. As every dual face  $f$  is part of exactly one zone of each type, we can also obtain target  $y$ - and  $z$ -coordinates in this way to obtain a target position  $t(f) = (t_x, t_y, t_z)$  for a dual face  $f$ . We then place the corner of  $f$  on the vertex  $v$  in  $f$  that minimizes  $\|p(v) - t(f)\|$ , where  $\|\cdot\|$  is the Euclidean norm.

*Connecting corners.* To complete the polycube layout, we simply need to connect any two adjacent corners  $c_1$  and  $c_2$ , separated by a single loop  $\ell$  in the dual structure, via a path on  $\mathcal{M}'$ . This path  $\pi$  cannot intersect/overlap with any other path between adjacent corners (except for in the corners itself), and may not intersect any other loop in the dual structure other than  $\ell$ . We generally want  $\pi$  to follow the edges of  $\mathcal{M}'$ , unless this is not possible (see below), and that  $\pi$  is as short as possible in terms of geometric length.

This task is equivalent to the layout embedding problem discussed by [Born et al. 2021]. However, given the fact that we already have a dual structure that heavily constrains the paths between corners, we believe that a greedy approach will also work well, and will likely avoid the bad scenarios highlighted in [Born et al. 2021].<sup>1</sup> Thus, we compute paths between corners one at a time, and forbid the edges and internal vertices of the computed paths to be used by future paths. Note that, similarly to when constructing the dual structure, we may run into a situation where no path between corners exists anymore. We therefore create a mesh  $\mathcal{M}^+$  that augments  $\mathcal{M}'$  with the edge graph  $G$  defined in Section 5.1 (additionally incorporating refinements from  $\mathcal{M}$  to  $\mathcal{M}'$ ). To construct  $\mathcal{M}^+$  we connect  $\mathcal{M}'$  to  $G$  by connecting every vertex  $v$  of  $\mathcal{M}'$  with the edge of  $\mathcal{M}'$  (represented by a vertex in  $G$ ) opposite of  $v$  in any triangle of  $\mathcal{M}'$  incident to  $v$ . If a computed path  $\pi$  between corners uses parts of  $G$ , then we add  $\pi$  to the original mesh  $\mathcal{M}'$ , and hence also expand  $G$  and  $\mathcal{M}^+$ . As a result, there will always exist a path between any two adjacent corners that satisfies the constraints.

### 5.3 Manual intervention

Our approach offers several possibilities for human users to intervene in the iterative process. When constructing the dual structure, a user can influence the loops to be added to the dual structure by selecting vertices of interest, the loop computation step can then be adapted to find a path through the vertices of interest. Furthermore,

<sup>1</sup>We have tried to use the publicly available implementation of [Born et al. 2021], but the implementation was prohibitively slow on our meshes.

users can decide the type of loop ( $X/Y/Z$ ) to be added, and/or the zone the loop is added. Similarly, users can select loops to be removed from the dual structure (which is only permitted if the dual structure remains valid).

In the primalization part of the algorithm, a user can change the position of a corner, and also edit the paths between two adjacent corners. Our dual structure makes it very clear which constraints must be satisfied to obtain a valid polycube layout (see Section 5.2).

In our current implementation we support user intervention by means of letting the user decide the type of loop to be added, and the zone to be split. The user can tweak the parameters ( $\rho$ ,  $\gamma$ ,  $W$ ) between iterations. The user has the possibility to select and remove loops. We help the user by showing the (number of) critical vertices in different zones, helping the user to determine a good place to add a new loop. The corresponding results are shown in Section 6.

## 6 RESULTS

We implemented the presented approach using the Rust programming language and the Bevy graphics engine. The source code of our implementation is publicly available online.<sup>2</sup> We evaluated our method on a diverse range of input meshes. The complete dataset of our input instances, a compilation of accessible benchmark models used in related work, is also publicly available online.<sup>3</sup> We used a wide range of meshes of genus 0 in our evaluation, with mesh complexity varying from 1,000 to 40,000 triangles. Since manual intervention is an important aspect of our approach, we demonstrate the results for different forms of manual intervention, and show that our approach can consistently produce valid high-quality polycube layouts, both fully automatically, and with (limited) human input.

*Loop selection strategies.* We first evaluate our algorithm running fully automatically, and compare loop selection strategies based on the four different criteria described in Section 5.1. The results are shown in Fig. 7. The *loop length* criterion results in loops that are very close to the initial loops, not capturing any geometric features. This criterion is useful to compute the initial loops, but should not be used in later stages, unless you combine it with any of the other criteria. The *loop distribution* criterion results in nicely distributed loops, capturing the main shape of the model. However, the fin on the side is not captured. The *critical count* criterion produces a similar result, also missing the fin. Finally, the *critical spread* criterion is able to capture smaller features such as the fin.

*Polycube layouts with minimal intervention.* In this evaluation we allow the user to choose only the type of the next loop to be added, and the best loop is then computed using the critical count criterion with  $\rho = 0.2$ . For the ‘bone’ model (see Fig. 8), the algorithm is able to correctly choose the zone that needs more refinement, gradually capturing the geometric features from large to small.

*Polycube layouts with manual intervention.* In our final evaluation we allow the user to choose the zone (and thus, also the type) where a loop needs to be added to the dual structure. These loops are then computed using either the loop distribution, critical spread, or critical count criterion, which can also be chosen by the user.

<sup>2</sup><https://github.com/maximsnoep/Polycube-Layouts-via-Iterative-Dual-Loops>

<sup>3</sup><https://github.com/maximsnoep/manimeshes>

Finally, the user is also given the ability to remove loops. The results for various meshes are shown in Fig. 9 (and also in Fig. 1).

The polycubes generated through our approach are visually similar to those produced by state-of-the-art methods. However, our method allows the user to have a lot of control in capturing relevant geometric features and determining the amount of detail in the resulting polycube layout. Also, it is very easy for the user to add new relevant loops, as they only need to choose a zone that needs refinement and determine the right quality criterion to compute the loop, avoiding the process of manually tracing the loops. Our approach successfully captures most, if not all, important geometric features of the models. Note that the polycube layouts themselves may not look very smooth, but this is caused by the fact that we restrict the layout paths to follow the mesh when possible. If necessary, this can easily be improved by refining the mesh further, or by tracing paths that do not strictly follow the edges of the mesh.

*Performance.* Although it is hard to measure the overall performance of our approach when manual intervention is involved, we briefly want to give an indication of how efficient our algorithm is. Overall, each of the presented polycube layouts took only minutes to construct using our implementation. Adding a single loop works in real-time for small models (with  $\sim 1,000$  triangles) and takes a few seconds for large models (with  $\sim 100,000$  triangles). The primalization step (which is currently fully automatic in our implementation) takes several minutes depending on the complexity of the dual structure. Note that our implementation is not optimized for performance, and that especially the primalization step can be heavily parallelized. Thus, our algorithm is quite efficient when compared to the state-of-the-art.

## 7 CONCLUSION

We have introduced a novel approach to polycube computation that is robust, flexible, and efficient. Using the dual representation of polycubes, our method natively supports iterative refinement with the option for manual intervention. We have implemented a basic version of this approach and demonstrated its effectiveness on multiple benchmark models. However, we think that further improvement is possible by using more sophisticated techniques for the individual steps of the algorithm.

*Computing loops.* Our current method of computing loops is based on shortest paths in specific weighted graphs. While this method is often effective in finding good loops for the dual structure, it may sometimes miss the opportunity to capture multiple relevant features of the mesh that should be captured by a single loop (for example, capturing both ears of the bunny in Fig. 1). Due to modeling this problem as a shortest-path problem, it is also non-trivial to resolve this issue by simply playing with the weights of the graph. Instead, we will first need to identify relevant features of the model, and then find a way to capture multiple of these features with a single loop if applicable, whilst also trying to minimize the resulting distortion. However, this will require a radically different approach.

*Primalization.* For the primalization we currently use a very simple greedy approach. First of all, when placing the corners, we are very strict in the alignment by computing a single target coordinate for each zone. This may be undesirable for certain models. Furthermore, the greedy approach of adding paths sometimes creates suboptimal embeddings of the paths around a single corner, as incident paths must adhere to a particular circular order. It may be worthwhile to investigate other existing approaches for polycube layouts and determine which one can be most effectively adapted to incorporate the constraints imposed by the dual structure.

*Orientation.* Our approach heavily relies on the initial orientation of the input model for computing the polycube layout. Currently we properly orient the models manually. It would be worthwhile to develop an automatic preprocessing step that orients the model to align well with the principal directions ( $X, Y, Z$ ), or to eliminate the reliance of our approach on the initial orientation.

*Higher genus models.* One major limitation of our current approach is its restriction to models of genus 0. We believe that our approach can be extended to higher genus models, but we will need to adapt two aspects of the algorithm. First of all, our iterative approach of adding loops one at a time cannot change the genus of the underlying model. Hence, we must adapt the initialization step to compute a dual structure that directly corresponds to a polycube of the right genus (see Fig. 6). Second, the conditions on a valid dual structure described in Section 4 have only been proven necessary and sufficient for meshes of genus 0. Therefore, we will also need to establish the proper conditions for higher genus models.

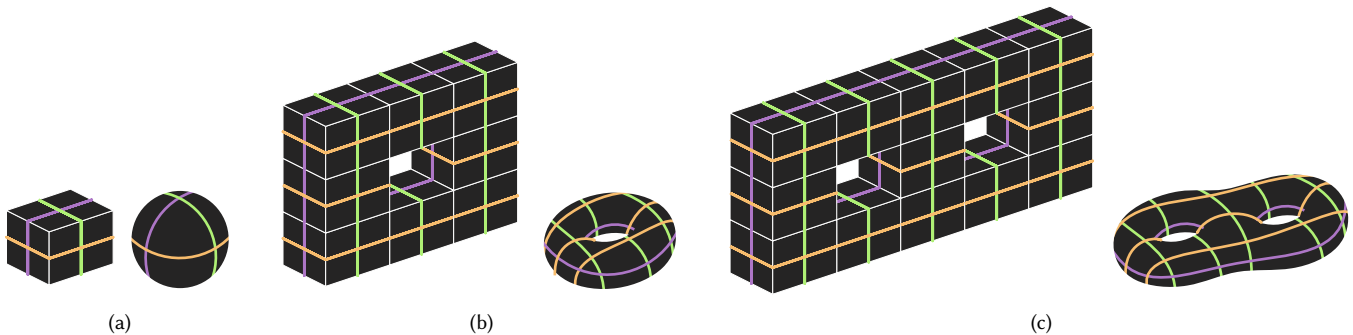


Fig. 6. Initialization based on the genus of the input model.

## REFERENCES

- Markus Baumeister and Leif Kobbelt. 2023. How close is a quad mesh to a polycube? *Computational Geometry* 111, Article 101978 (April 2023), 22 pages. <https://doi.org/10.1016/j.comgeo.2022.101978>
- Therese Biedl and Burkay Genc. 2004. When can a graph form an orthogonal polyhedron?. In *Proceedings of the 16th Canadian Conference on Computational Geometry* (Montreal, Quebec, Canada) (CCC'04), 53–56. <http://www.ccg.ca/proceedings/2004/15.pdf>
- Janis Born, Patrick Schmidt, and Leif Kobbelt. 2021. Layout Embedding via Combinatorial Optimization. *Computer Graphics Forum* 40, 2 (May 2021), 277–290. <https://doi.org/10.1111/cgf.142632>
- Marcel Campen, David Bommes, and Leif Kobbelt. 2012. Dual Loops Meshing: Quality Quad Layouts on Manifolds. *ACM Transactions on Graphics* 31, 4, Article 110 (July 2012), 11 pages. <https://doi.org/10.1145/2185520.2185606>
- Gianmarco Cherchi, Marco Livesu, and Riccardo Scateni. 2016. Polycube Simplification for Coarse Layouts of Surfaces and Volumes. *Computer Graphics Forum* 35, 5 (Aug. 2016), 11–20. <https://doi.org/10.1111/cgf.12959>
- Corentin Dumery, François Protais, Sébastien Mestrallet, Christophe Bourcier, and Franck Ledoux. 2022. Evocube: A Genetic Labelling Framework for Polycube-Maps. *Computer Graphics Forum* 41, 6 (Sept. 2022), 467–479. <https://doi.org/10.1111/cgf.14649>
- David Eppstein and Elena Mumford. 2010. Steinitz Theorems for Orthogonal Polyhedra. In *Proceedings of the Twenty-Sixth Annual Symposium on Computational Geometry* (Snowbird, Utah, USA) (SoCG '10). Association for Computing Machinery, New York, NY, USA, 429–438. <https://doi.org/10.1145/1810959.1811030>
- Xianzhong Fang, Weiwei Xu, Hujun Bao, and Jin Huang. 2016. All-Hex Meshing Using Closed-Form Induced Polycube. *ACM Transactions on Graphics* 35, 4, Article 124 (July 2016), 9 pages. <https://doi.org/10.1145/2897824.2925957>
- Xiao-Ming Fu, Chong-Yang Bai, and Yang Liu. 2016. Efficient Volumetric PolyCube-Map Construction. *Computer Graphics Forum* 35, 7 (Oct. 2016), 97–106. <https://doi.org/10.1111/cgf.13007>
- Ismael Garcia, Jiazhi Xia, Ying He, Shi-Qing Xin, and Gustavo Patow. 2013. Interactive Applications for Sketch-Based Editable Polycube Map. *IEEE Transactions on Visualization and Computer Graphics* 19, 7 (July 2013), 1158–1171. <https://doi.org/10.1109/TVCG.2012.308>
- James Gregson, Alla Sheffer, and Eugene Zhang. 2011. All-Hex Mesh Generation via Volumetric Polycube Deformation. *Computer Graphics Forum* 30, 5 (Aug. 2011), 1407–1416. <https://doi.org/10.1111/j.1467-8659.2011.02015.x>
- Hao-Xiang Guo, Xiaohan Liu, Dong-Ming Yan, and Yang Liu. 2020. Cut-Enhanced PolyCube-Maps for Feature-Aware All-Hex Meshing. *ACM Transactions on Graphics* 39, 4, Article 106 (Aug. 2020), 14 pages. <https://doi.org/10.1145/3386569.3392378>
- Ying He, Hongyu Wang, Chi-Wing Fu, and Hong Qin. 2009. A divide-and-conquer approach for automatic polycube map construction. *Computers & Graphics* 33, 3 (June 2009), 369–380. <https://doi.org/10.1016/j.cag.2009.03.024>
- Kangkang Hu and Yongjie Jessica Zhang. 2016. Centroidal Voronoi tessellation based polycube construction for adaptive all-hexahedral mesh generation. *Computer Methods in Applied Mechanics and Engineering* 305 (June 2016), 405–421. <https://doi.org/10.1016/j.cma.2016.03.021>
- Jin Huang, Tengfei Jiang, Zeyun Shi, Yiyang Tong, Hujun Bao, and Mathieu Desbrun. 2014.  $\ell_1$ -Based Construction of Polycube Maps from Complex Shapes. *ACM Transactions on Graphics* 33, 3, Article 25 (June 2014), 11 pages. <https://doi.org/10.1145/2602141>
- Lingxiao Li, Paul Zhang, Dmitriy Smirnov, S. Mazdak Abulnaga, and Justin Solomon. 2021. Interactive All-Hex Meshing via Cuboid Decomposition. *ACM Transactions on Graphics* 40, 6, Article 256 (Dec. 2021), 17 pages. <https://doi.org/10.1145/3478513.3480568>
- Juncong Lin, Xiaogang Jin, Zhengwen Fan, and Charlie C. L. Wang. 2008. Automatic Polycube-Maps. In *Proceedings of the 5th International Conference on Advances in Geometric Modeling and Processing* (Hangzhou, China) (GMP'08). Springer-Verlag, Berlin, Heidelberg, 3–16. [https://doi.org/10.1007/978-3-540-79246-8\\_1](https://doi.org/10.1007/978-3-540-79246-8_1)
- Marco Livesu, Nico Pietroni, Enrico Puppo, Alla Sheffer, and Paolo Cignoni. 2020. LoopyCuts: Practical Feature-Preserving Block Decomposition for Strongly Hex-Dominant Meshing. *ACM Transactions on Graphics* 39, 4, Article 121 (Aug. 2020), 17 pages. <https://doi.org/10.1145/3386569.3392472>
- Marco Livesu, Nicholas Vining, Alla Sheffer, James Gregson, and Riccardo Scateni. 2013. Polycut: Monotone Graph-Cuts for Polycube Base-Complex Construction. *ACM Transactions on Graphics* 32, 6, Article 171 (Nov. 2013), 12 pages. <https://doi.org/10.1145/2508363.2508388>
- Ivan Malcev. 2011. Automated Blocking for Structured CFD Gridding with an Application to Turbomachinery Secondary Flows. In *20th AIAA Computational Fluid Dynamics Conference* (Honolulu, Hawaii, USA). American Institute of Aeronautics and Astronautics, Reston, VA, USA, Article 2011-3049, 14 pages. <https://doi.org/10.2514/6.2011-3049>
- Manish Mandad, Ruizhi Chen, David Bommes, and Marcel Campen. 2022. Intrinsic mixed-integer polycubes for hexahedral meshing. *Computer Aided Geometric Design* 94, Article 102078 (March 2022), 15 pages. <https://doi.org/10.1016/j.cagd.2022.102078>
- Sébastien Mestrallet, François Protais, Christophe Bourcier, and Franck Ledoux. 2023. Limits and prospects of polycube labelings. In *SIAM International Meshing Roundtable Workshop 2023* (Amsterdam, The Netherlands) (SIAM IMR23), 5 pages. <https://internationalmeshingroundtable.com/assets/research-notes/imr31/2012-comp.pdf>
- Nico Pietroni, Marcel Campen, Alla Sheffer, Gianmarco Cherchi, David Bommes, Xifeng Gao, Riccardo Scateni, Franck Ledoux, Jean Remacle, and Marco Livesu. 2022. Hex-Mesh Generation and Processing: A Survey. *ACM Transactions on Graphics* 42, 2, Article 16 (Oct. 2022), 44 pages. <https://doi.org/10.1145/3554920>
- Nico Pietroni, Enrico Puppo, Giorgio Marcias, Roberto Scopigno, and Paolo Cignoni. 2016. Tracing Field-Coherent Quad Layouts. *Computer Graphics Forum* 35, 7 (Oct. 2016), 485–496. <https://doi.org/10.1111/cgf.13045>
- François Protais, Maxence Reberol, Nicolas Ray, Ettiene Corman, Franck Ledoux, and Dmitry Sokolov. 2022. Robust Quantization for Polycube Maps. *Computer-Aided Design* 150, Article 103321 (Sept. 2022), 11 pages. <https://doi.org/10.1016/j.cad.2022.103321>
- Dmitry Sokolov and Nicolas Ray. 2015. *Fixing normal constraints for generation of polycubes*. Research Report. LORIA. <https://inria.hal.science/hal-01211408>
- Marco Tarini, Kai Hormann, Paolo Cignoni, and Claudio Montani. 2004. Polycube-Maps. *ACM Transactions on Graphics* 23, 3 (Aug. 2004), 853–860. <https://doi.org/10.1145/1015706.1015810>
- Shenghua Wan, Zhao Yin, Kang Zhang, Hongchao Zhang, and Xin Li. 2011. A topology-preserving optimization algorithm for polycube mapping. *Computers & Graphics* 35, 3 (June 2011), 639–649. <https://doi.org/10.1016/j.cag.2011.03.018>
- Hongyu Wang, Miao Jin, Ying He, Xianfeng Gu, and Hong Qin. 2008. User-Controllable Polycube Map for Manifold Spline Construction. In *Proceedings of the 2008 ACM Symposium on Solid and Physical Modeling* (Stony Brook, New York, USA) (SPM'08). Association for Computing Machinery, New York, NY, USA, 397–404. <https://doi.org/10.1145/1364901.1364958>
- Jiazhi Xia, Ismael Garcia, Ying He, Shi-Qing Xin, and Gustavo Patow. 2011. Editable Polycube Map for GPU-Based Subdivision Surfaces. In *Symposium on Interactive 3D Graphics and Games* (San Francisco, California, USA) (I3D '11). Association for Computing Machinery, New York, NY, USA, 151–158. <https://doi.org/10.1145/1944745.1944771>
- Yang Yang, Xiao-Ming Fu, and Ligang Liu. 2019. Computing Surface PolyCube-Maps by Constrained Voxelization. *Computer Graphics Forum* 38, 7 (Nov. 2019), 299–309. <https://doi.org/10.1111/cgf.13838>
- Wuyi Yu, Kang Zhang, Shenghua Wan, and Xin Li. 2014. Optimizing polycube domain construction for hexahedral remeshing. *Computer-Aided Design* 46 (Jan. 2014), 58–68. <https://doi.org/10.1016/j.cad.2013.08.018>
- Hui Zhao, Xuan Li, Wencheng Wang, Xiaoling Wang, Shaodong Wang, Na Lei, and Xiangfeng Gu. 2019. Polycube Shape Space. *Computer Graphics Forum* 38, 7 (Nov. 2019), 311–322. <https://doi.org/10.1111/cgf.13839>



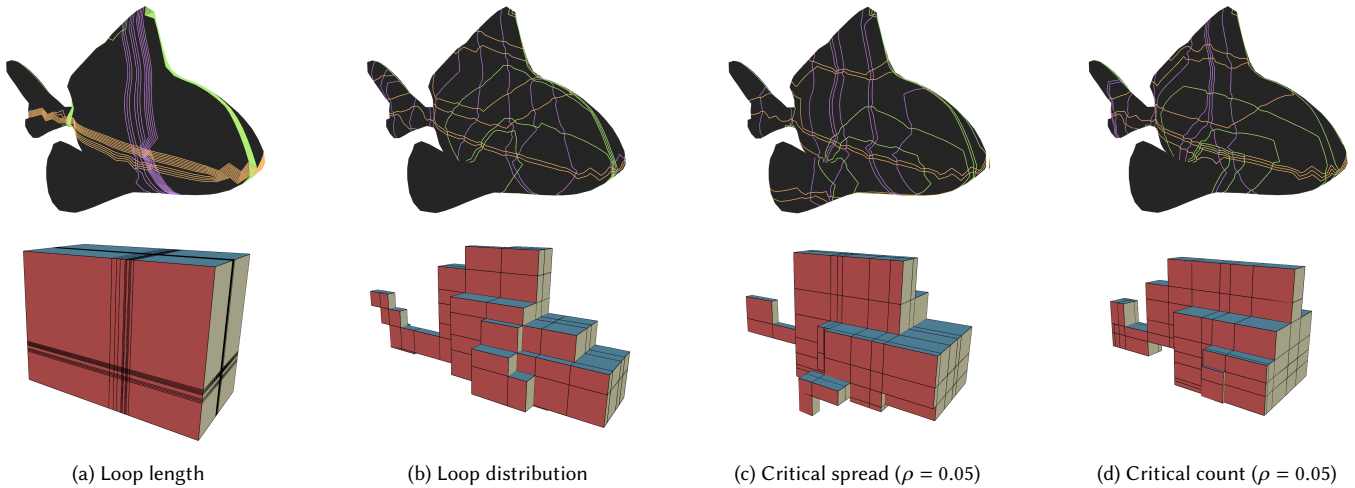


Fig. 7. Comparison of our 4 loop selection criteria methods for iterative loop selection on the ‘blub001k’ model. The automatic method used 10 iterations for X/Y/Z (30 loops in total). Each iteration sampled 200 loops with  $\gamma = 1.0$ . Then the best loop was selected by the loop criteria: Loop length (a), loop distribution (b), critical spread (c), and critical count (d). Both the loop structure and the corresponding polycube are shown. (each example was initialized using the loop length criterion with 2000 samples and  $\gamma = 1.0$ )

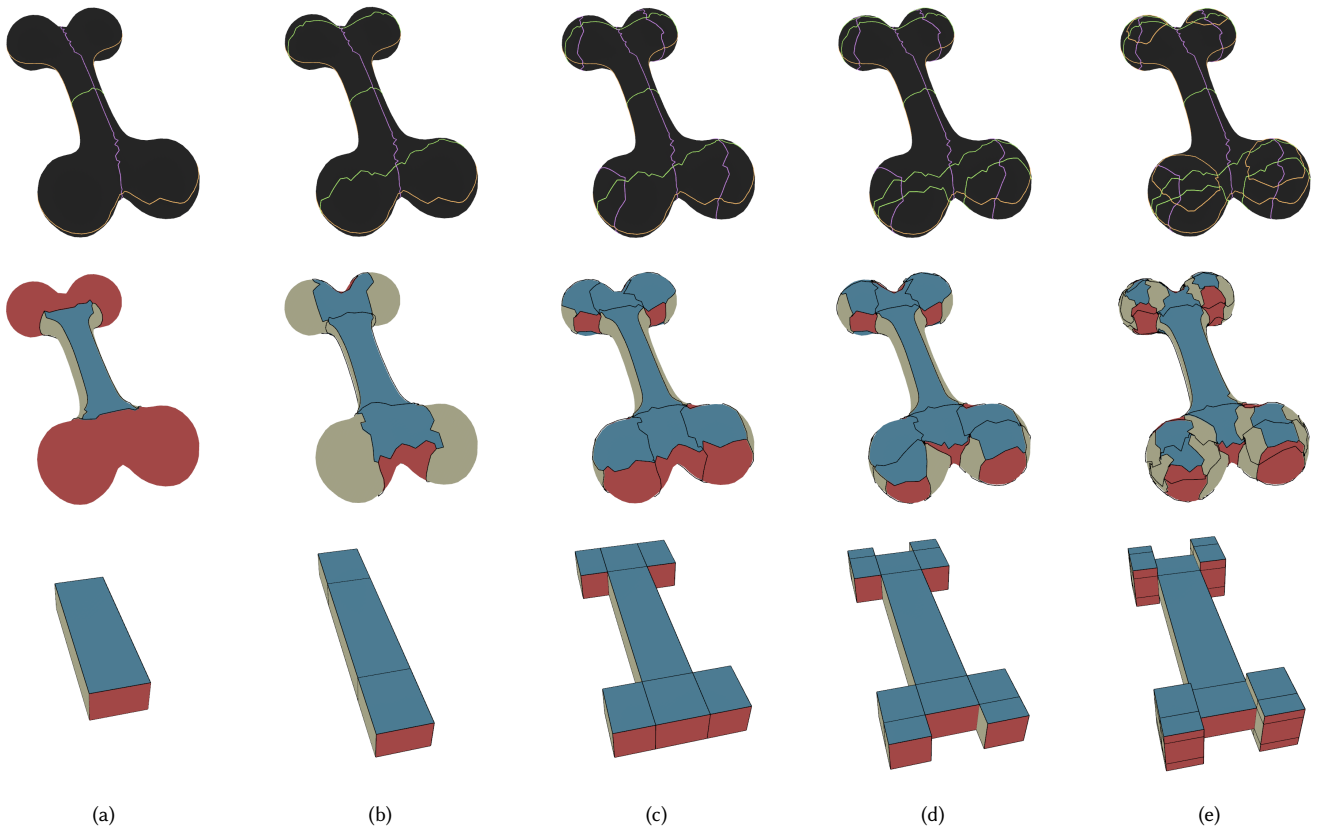


Fig. 8. Snapshots of our presented iterative approach on the ‘bone’ model. The implementation finds an initial solution (a), three interleaving loops selected via the critical spread criteria with 2000 samples,  $\gamma = 1.0$ , and  $\rho = 0.2$ . In (b) through (e), the automated process chooses the next zones to add loops, based on the number of critical points in each zone, and adds the best loop via the critical spread criteria with 500 samples,  $\gamma = 1.0$ , and  $\rho = 0.2$ . We used  $W = 50$  during primalization.

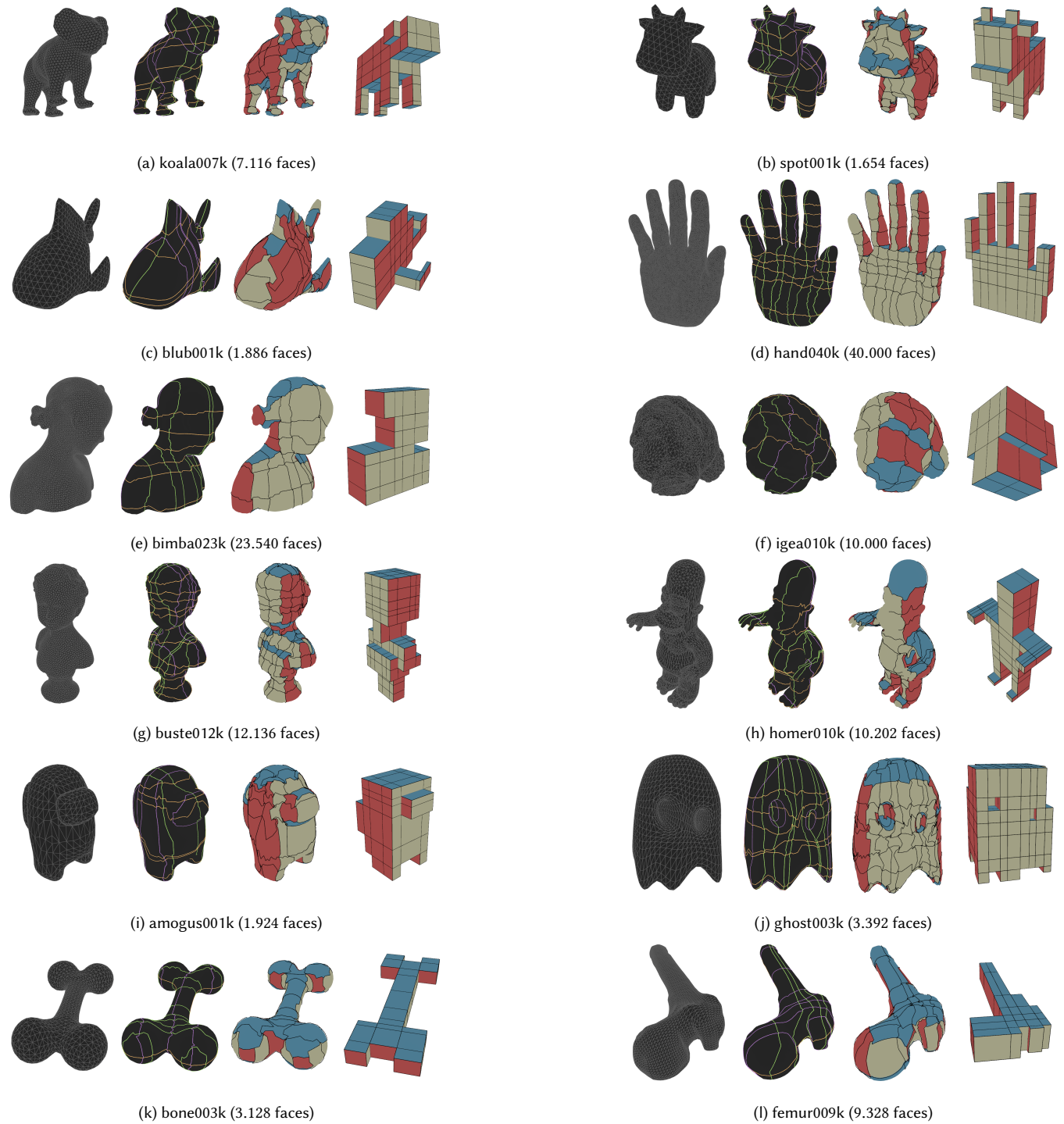


Fig. 9. A collection of polycube layouts generated through our approach. Each set shows four distinct visual representations: (1) the original input mesh, (2) the computed dual structure, (3) the primalized version of the dual structure, representing the polycube layout, and (4) the final polycube corresponding to the layout. The initial loops were computed using the loop length criteria with 2000 samples and  $\gamma = 1.0$ . The iterative loops were computed using user specified loop selection criteria with 200 samples and  $\gamma = 1.0$ . The value for  $\rho$  was tweaked per model per iteration, but remained in the range of 0.1 to 0.5. We used  $W = 50$  during the primalization.